LSMO-STO(110) Multilayered Structure Grown by Metalorganic Aerosol Deposition

Oleg SAPOVAL[1], Alexander BELENCHUK[1], Valeriu CANTER[1], Efim ZASAVITSKY[1], Vasily MOSHNYAGA[2]

[1]*IEEN,Academy of Sciences of Moldova, sapoval@nano.asm.md*
[2]*I. Physikalisches Institut, Georg-August-Universitat-Gottingen, Germany,*

***Abstract* —$La_{0.67}Sr_{0.33}MnO_3$-$SrTiO_3$ multilayered structure was grown on $SrTiO_3$(110) substrates by metalorganic aerosol deposition technique. The crystal structure was examined by X-ray analysis including simulation of diffraction and reflection patterns. The magnetotransport properties of superlattice are presented. The critical thickness of (110)-oriented LSMO layers is lower than 7 perovskite unite cells. The oxygen stoichiometry provided due to high gas pressure conditions is responsible for reducing of critical thickness of LSMO layers at LSMO-STO(110) interfaces.**

***Index Terms* — manganites based superlattice, metalorganic aerosol deposition, simulations of X-ray diffraction and scattering.**

I. INTRODUCTION

$La_{0.67}Sr_{0.33}MnO_3$ (LSMO) still remains among of manganites the best candidate for the electrode material of spintronic devices because of its 100% spin polarization at room temperatures. One of the obstacles for realization its high potential is the difference in magnetic properties at interfaces and bulk of the film [1]. The widely used for manganites epitaxy $SrTiO_3$ (STO) substrate has (100) orientation. The polar discontinuity at interface LSMO-STO along (100) planes is possible reason of "dead" layer formation. Interface between TiO_2-terminated STO substrate and LSMO film is constructed from charged $La_{1-x}Sr_xO$ and neutral TiO_2 planes that lead to electronic redistribution. This problem will be inherited by numerous interfaces of LSMO-STO superlattice (SL) grown on (100) oriented substrate. Tailoring interface along (110) plane allows to escape polar catastrophe due to stacking neutral bilayers ($SrTiO^{4+}$ – O_2^{4-}) and ($La_{0.67}Sr_{0.33}MnO^{4+}$ – O_2^{4-})[2]. The interest to (110) oriented LSMO films grown on STO substrates recently was stirred up by demonstration of high temperature (560 K) ferromagnetism in ultrathin layer [3]. For spintronic applications the ferromagnetic electrodes have to be epitaxial and atomically flat. Recently was demonstrated persistent layer-by-layer growth of atomically flat LSMO(110) films [4].

The LSMO-STO(100) SLs were extensively investigated whereas to the best of our knowledge a work was presented on LSMO-STO(110) SL only [5].

The STO films used as insulating layers in tunneling magnetoresistance devices produced by widely spread PLD and MBE techniques reveal stoichiometry problem [6]. Oxygen vacancies act as shallow donors giving rise to a leakage through spacer layer.

Metalorganic aerosol deposition (MAD) technique [7] provides oxygen stoichiometry due to high oxygen pressures growth conditions.

The goal of presented work was to prepare by MAD technique LSMO-STO multilayered structure on (110) oriented STO substrate and characterize it structure and magnetotransport properties.

II. EXPERIMENT

The LSMO-STO superlattice was grown by MAD technique on STO(110) substrate heated to T_{sub}=950 °C. Epitaxial multilayered structure was formed in result of sequential spraying of aerosols of 2 organic solutions containing metalorganic precursors. LSMO layers grew from mixture of La-, Sr-, Mn-acetylacetonates and STO layers were derived from Sr-acetylacetonate and Ti-isopropoxide. Cation stoichiometry in layers was achieved during preliminary depositions of single films by optimization of precursors proportion in solutions. The oxygen stoichiometry is assumed to provide due to a high (PO_2~0.21 atm) gas pressure conditions. Deposition chamber was equipped by ellipsometry measurement system for monitoring of the growth process. The monolayer accuracy was achieved by accurate calibration of dosing units.

Time diagram of the growth of first two superlattice periods is presented on Fig. 1. Ellipsometry signal reflects the stages of LSMO and STO growth synchronized with operation of syringe dosing units. The growth of first 4 LSMO monolayers (ML - 0.274 nm in (110) direction) on STO surface is clearly defined on initial growth stage.

The structure was composed from 7 LSMO layers of 4 nm thick separated by about 2 nm STO layers and finished by additional LSMO layer.

The film and substrate surface morphology was characterized by scanning probe microscopy (SPM) including atomic force microscopy (AFM) for insulating and scanning tunneling microscopy (STM) for conducting samples. The crystal parameters of grown structure were characterized by a small-angle x-ray reflectivity (XRR) and X-ray diffraction (XRD) performed in a Siemens D5000 diffractometer. Transport measurements were performed by standard 4-probe technique using commercial PPMS from "Quantum Design".

Magnetization was measured by means of commercial SQUID (MPMS, "Quantum Design").

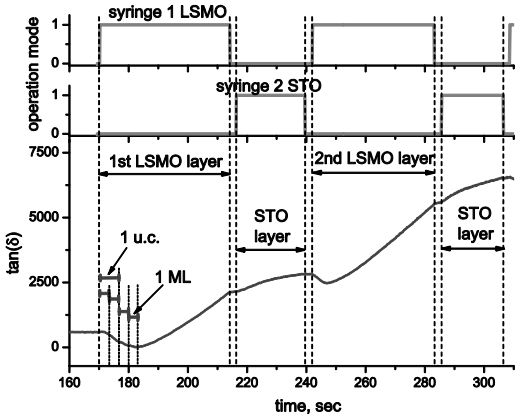

Fig. 1 Time diagram of the growth process. The ellipsometry signal tan(δ) characterization of the first two LSMO-STO pairs growth. Mark 1 u.c. corresponds to deposition of a lattice parameter layer in (110) direction. Marks 1 ML correspond to growth of a LSMO monolayer. Syringe operation mode indicates: 0-0 feeding speed, 1-full feeding speed.

III. RESULTS AND DISCURSION

SPM surface analysis is presented on Fig. 2. Surface of STO(110) substrate after annealing at 950°C clearly demonstrates terraces of about 20-100 nm width and a monolayer height (~0.276 nm). Rectangular form of terraces is specified by slight miscut angle away from exact (110) oriented surface. The measured mean square roughness (RMS) is 0.14 nm.

First LSMO layer of 4 nm thick inherits terrace structure from substrate, but terrace steps are no longer clearly visible. The surface is still atomically smooth with RMS=0.21 nm. Relief of the layer is formed by small (about a few nanometers) secondary terraces.

The crystal structure of LSMO-STO multilayered structure was examined by X-ray analysis. Fig.3 (a) shows θ-2θ X-ray diffraction spectra measured around the (110) Bragg peak for the LSMO-STO SL. The evidence for a SL formation is confirmed by well-formed satellite peaks up to 6th order in XRR and 2nd order in XRD pattern. The SL periods were calculated from satellite peak positions using standard procedure.

The SL period T can be accurately determined from the equation $(2\sin\theta_{SLn}-2\sin\theta_{SL0})=\pm n\lambda/T$, where λ is the X-ray wavelength, n is the order of satellite peaks, θ_{SLn} is the diffraction angle of the satellite peak, and θ_{SL0} is the Bragg angle of the host lattice. Calculated period is equal to 5.47 nm. The θ_{SL0} peak position is shifted to the right from (110) substrate peak reflecting the strain of out-of-plane lattice parameter. To estimate strain parameter Δa/a we assume the Mn-Mn distances in [100] and [010] direction in the strained LSMO will be the same as in unstrained LSMO. Then expected out-of-plane lattice parameter of LSMO layer on STO(110) will be a=0.2726 nm and Δa/a=0.0123.

Period calculated from XRR data (Fig. 3 (b)) is differ from defined from XRD one. Extrapolation of dependence of interlayer distance $d=n\lambda/2\sin\theta_{SLn}$ from $1/\sin^2\theta_{SLn}$ to zero gives us period value T=5.75 nm.

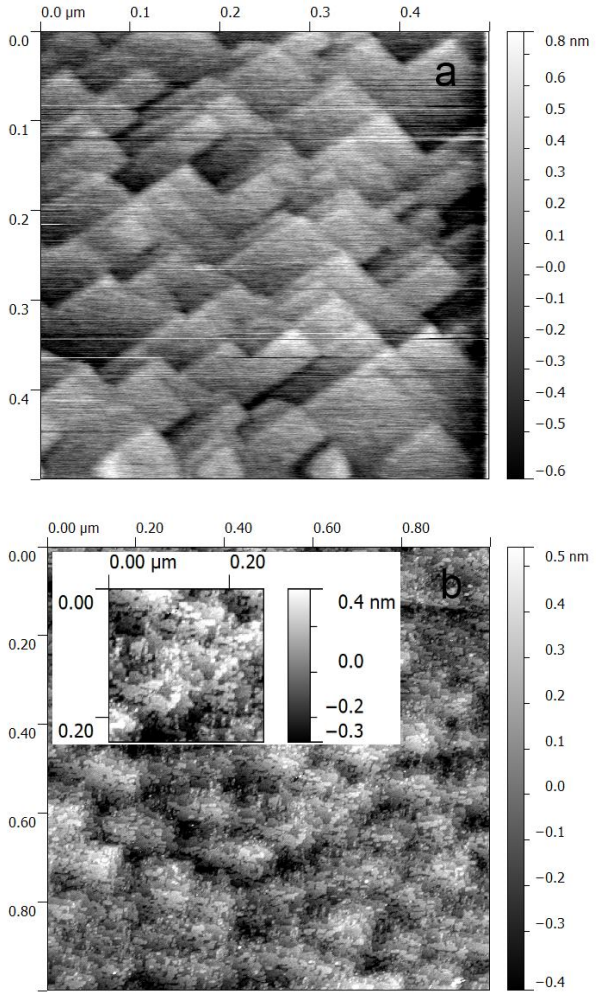

Fig. 2 SPM images of (a) STO(110) substrate annealed surface (AFM) and (b) surface after deposition of LSMO 4 nm thick layer (STM). Insert in (b) reveals 2D growth mode.

The difference in calculated periods can be explained from origin of satellites peaks on XRR and XRD patterns. In XRD case oscillations emerge from the crystalline structure, while in XRR fringes originate from the presence of two interfaces, independent of the crystallinity of the material in between. Consequently, the XRD fringes are extremely sensitive on the qualities of the interface while the Laue oscillations depend only weakly on properties like surface roughness but are sensitive to crystalline disorder. Therefore, the two provide complementary information: the XRR fringes determine the total thickness of a sample, while the XRD oscillations probe the size of the crystalline ordered volume.

The simulations of XRD and XRR curves were performed using *TER_SL on the WEB: X-ray specular reflection from multilayers with rough interfaces* and *GID_SL on the WEB: Dynamical X-ray diffraction from strained crystals, multilayers and SL* [8]. In simulation routine were used the parameters calculated from experimental curve. Due to small number of repetition (7 periods) the structure were presented as 15 individual layers with their own parameters (Table 1).

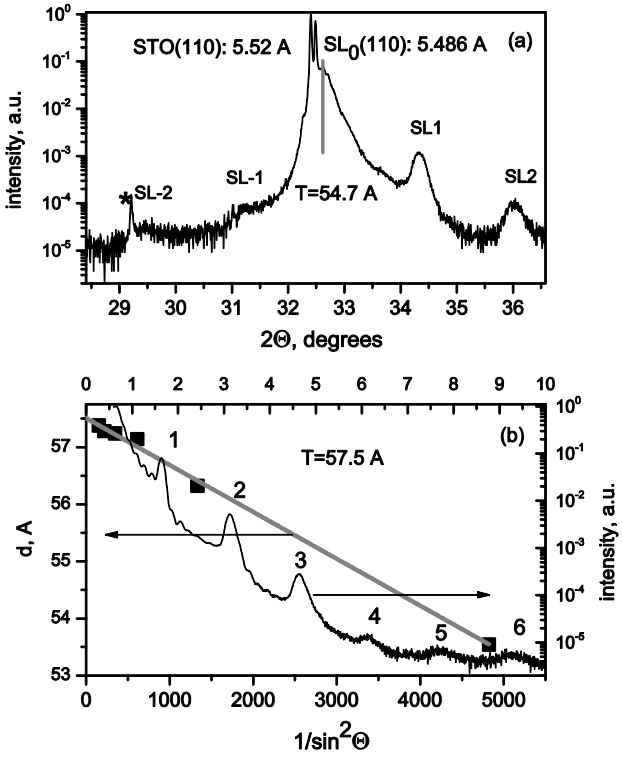

Fig. 3 (a) Experimental X-ray diffraction spectrum around (110) Bragg's peak of the $La_{0.67}Sr_{0.33}MnO_3$-$SrTiO_3$ multilayered structure with period 5.47 nm. Asterisk denotes CuK_β line STO(110) (b) The small angle X-ray reflection pattern and the plot of interlayer distance d vs $1/\sin^2\theta_n$ for $La_{0.67}Sr_{0.33}MnO_3$-$SrTiO_3$ multilayered structure. The intercept of the extrapolated line with the d axis shows the SL period.

The individual thicknesses of component were taken into account around mean value of period. Adjusting curves were performed by variation individual thicknesses, strain parameter (Δa/a) and roughness. The roughness was gradually increased from 0.14 nm for bottom layer to 0.7 nm for top layer as specified for substrate and whole structure from SPM measurement. The reasonable roughness parameters didn't give satellite peaks intensity on simulated curves matched to experimental one. Introducing the "fraction" parameter reflected the presence of macro defects in grown SL improves intensity peaks ratio. We assume the uniform strain in LSMO layers across whole structure. The Δa/a parameter 0.012 used in simulations is in good agreement with estimated above. The individual thicknesses of layers used in XRR simulations were increased comparatively to that for XRD fitting to provide matching with larger period defined from experiment.

Thus, according to X-ray analysis the LSMO-STO multilayered structure was composed from 7 pairs of epitaxial 4 nm strained LSMO and free 1.7 nm STO layers. The thickness of LSMO layers (about 7 perovskite unit cells) lies below critical thickness above which the change of strain relaxation mechanism takes place [3].

Fig.5 presents magnetotransport properties of LSMO-STO SL grown on STO(110) substrate.

Table 1 The individual layers parameters used in simulation XRD curve for LSMO-STO multilayered structure.

Nr	Thickness	Δa/a	#	Roughness, A	Layer	Fraction
1	37.0	-0.120E-01		7.0	LSMO	0.85
2	17.0	0.000E+00		6.5	STO	0.90
3	37.5	-0.120E-01		6.0	LSMO	0.90
4	17.0	0.000E+00		5.5	STO	0.90
5	38.0	-0.120E-01		5.0	LSMO	0.90
6	17.0	0.000E+00		4.5	STO	0.90
7	38.5	-0.120E-01		4.2	LSMO	1.00
8	17.0	0.000E+00		3.9	STO	1.00
9	39.0	-0.120E-01		3.6	LSMO	1.00
10	17.0	0.000E+00		3.3	STO	1.00
11	39.5	-0.120E-01		3.0	LSMO	1.00
12	17.0	0.000E+00		2.7	STO	1.00
13	39.5	-0.120E-01		2.5	LSMO	1.00
14	17.5	0.000E+00		2.3	STO	1.00
15	40.0	-0.120E-01		2.1	LSMO	1.00
16	0.0	0.000E+00		1.4	STO	1.00

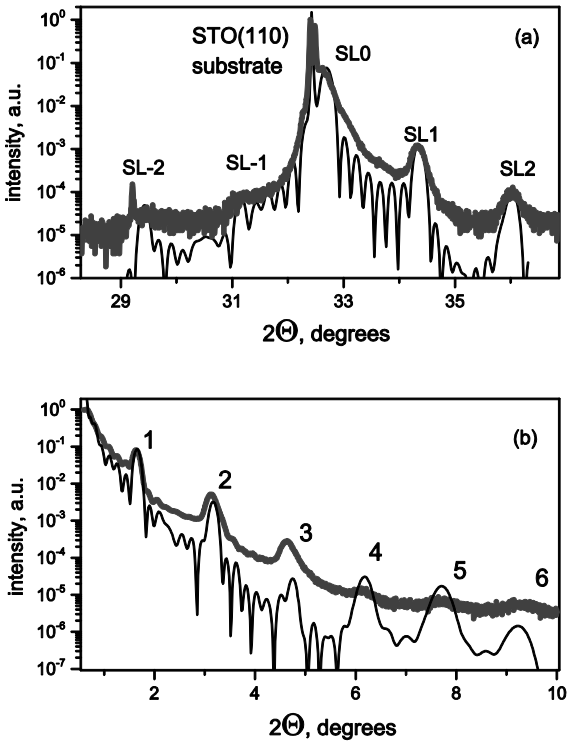

Fig. 4 Experimental (dark grey) and simulated (black) XRD (a) and XRR (b) curves for $La_{0.67}Sr_{0.33}MnO_3$-$SrTiO_3$ multilayered structure.

The multilayered structure resistance can be presented as parallel connected resistance of conducting LSMO layers. The crystal quality of subsequent layers decreases as follows from X-ray analysis and therefore the growth of resistance of LSMO layers is expected. The resistance of LSMO-STO structure was found to be about 3 times lower than the sum resistance of eight 4 nm LSMO layers and doesn't demonstrates insulating behavior as expected from chosen thickness of LSMO layers.

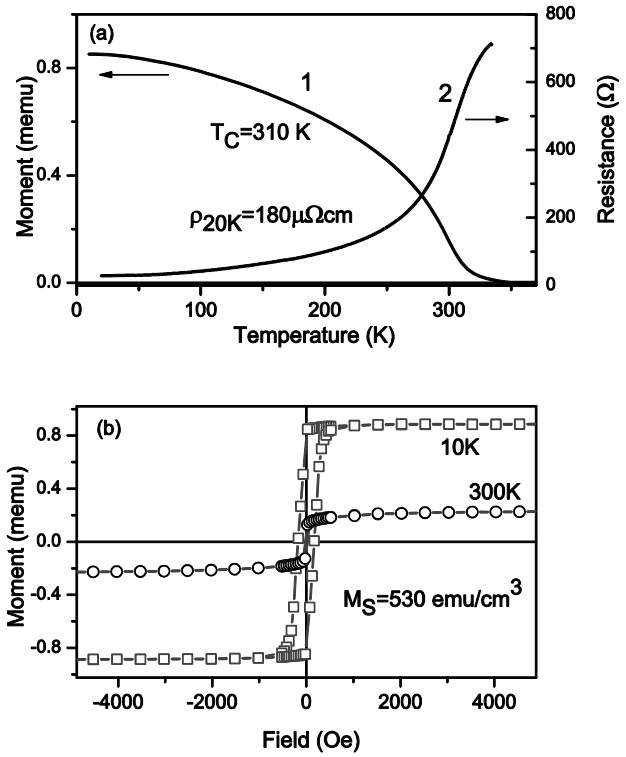

Fig. 5 Magnetic and transport properties of $La_{0.67}Sr_{0.33}MnO_3$-$SrTiO_3$ multilayered structure: (a) temperature dependence of magnetization (1) and resistance (2); (b) magnetic hysteresis loops measured at 10 K and 300 K.

Curie temperature of our structure is higher than that for ultra thin LSMO (110)-oriented layers. Saturation magnetization M_S related to sum of thicknesses of LSMO layers defined from XRR gives value of 530 emu/cm^3 or 3.43 μ_B/Mn. Whereas M_S associated with crystalline ordered volume of LSMO yields value 560 emu/cm^3 that is closer to magnetization of optimal doped "bulk" LSMO films. The coercive field H_c ~170 Oe (10 K) and 20 Oe (300K) indicates taking into account growth direction the magnetic homogeneity of structure.

Resistivity and magnetization of 8 LSMO layer composed in SL are inconsistent with results obtained for critical thickness in [3] and are in agreement with work [5]. We suppose that in ultra thin LSMO(110) layers the critical thickness can be sufficiently lower than 10 perovskite unite cells. In our experiment SL was grown at oxygen pressure about 3 orders greater then MBE can provide at comparable growth rate. Oxygen stoichiometry of manganite as well as titanite can be responsible for formation of critical layers at interfaces LSMO-STO(110).

IV. CONCLUSION

We have shown that MAD prepared LSMO-STO (110)-oriented SL has comparable crystal quality with prepared by MBE one. Observed difference in magnetotransport properties MAD and PLD deposited samples can be result of significantly higher oxygen pressure condition during sample growth.

ACKNOWLEDGMENTS

The authors acknowledge the S.Stepanov's project X-Ray Server provided free online access to X-ray data analysis programs. This work was supported by DFG (SFB 602) and STCU grant 5390.

REFERENCES

[1] J. J. Kavich, M. P. Warusawithana, J. W. Freeland, P. Ryan, X. Zhai, R. H. Kodama, and J. N. Eckstein, "Nanoscale suppression of magnetization at atomically assembled manganite interfaces: XMCD and XRMS measurements," *Phys. Rev. B*, vol. 76, no. 1, p. 014410, Jul. 2007.

[2] H. Boschker, J. Kautz, E. P. Houwman, G. Koster, D. H. A. Blank, and G. Rijnders, "Magnetic anisotropy and magnetization reversal of $La_{0.67}Sr_{0.33}MnO_3$ thin films on $SrTiO_3$(110)," *Journal of Applied Physics*, vol. 108, no. 10, pp. 103906–103906–6, Nov. 2010.

[3] H. Boschker, J. Kautz, E. P. Houwman, W. Siemons, D. H. A. Blank, M. Huijben, G. Koster, A. Vailionis, and G. Rijnders, "High-Temperature Magnetic Insulating Phase in Ultrathin $La_{0.67}Sr_{0.33}MnO_3$ Films," *Phys. Rev. Lett.*, vol. 109, no. 15, p. 157207, Oct. 2012.

[4] R. Bachelet, D. Pesquera, G. Herranz, F. Sánchez, and J. Fontcuberta, "Persistent two-dimensional growth of (110) manganite films," *Applied Physics Letters*, vol. 97, no. 12, pp. 121904–121904–3, Sep. 2010.

[5] J. X. Ma, X. F. Liu, T. Lin, G. Y. Gao, J. P. Zhang, W. B. Wu, X. G. Li, and J. Shi, "Interface ferromagnetism in (110)-oriented $La_{0.7}Sr_{0.3}MnO_3/SrTiO_3$ ultrathin superlattices," *Phys. Rev. B*, vol. 79, no. 17, p. 174424, May 2009.

[6] C. M. Brooks, L. F. Kourkoutis, T. Heeg, J. Schubert, D. A. Muller, and D. G. Schlom, "Growth of homoepitaxial $SrTiO_3$ thin films by molecular-beam epitaxy," *Applied Physics Letters*, vol. 94, no. 16, pp. 162905–162905–3, Apr. 2009.

[7] K. Gehrke, V. Moshnyaga, K. Samwer, O. I. Lebedev, J. Verbeeck, D. Kirilenko, and G. Van Tendeloo, "Interface controlled electronic variations in correlated heterostructures," *Phys. Rev. B*, vol. 82, no. 11, p. 113101, Sep. 2010.

[8] S. Stepanov, "TER_SL on the WEB, GID_SL on the WEB." http://www.sergey.gmca.aps.anl.gov.